Auger recombination and carrier multiplication in embedded silicon and germanium nanocrystals

C. Sevik and C. Bulutay
Department of Physics, Bilkent University, Bilkent, Ankara 06800, Turkey
(Received 10 December 2007; published 14 March 2008)

For Si and Ge nanocrystals (NCs) embedded in wide band-gap matrices, the Auger recombination and carrier multiplication (CM) lifetimes are computed exactly in a three-dimensional real space grid using empirical pseudopotential wave functions. Our results in support of recent experimental data offer other predictions. We extract simple Auger constants valid for NCs. We show that both Si and Ge NCs can benefit from photovoltaic efficiency improvement via CM due to the fact that under an optical excitation exceeding twice the band-gap energy, the electrons gain lion's share from the total excess energy and can cause a CM. We predict that CM becomes especially efficient for hot electrons with an excess energy of about 1 eV above the CM threshold.

DOI: 10.1103/PhysRevB.77.125414 PACS number(s): 73.22.−f, 72.20.Jv

I. INTRODUCTION

In the group IV semiconductor, Si and, to a lesser extent, Ge have been indispensable for the electronics and photovoltaics industry. The recent research efforts have shown that their nanocrystals (NCs) bring new features which fortify their stands. For instance, NCs can turn these indirect band-gap bulk materials into light emitters[1] or offer increased efficiencies in solar cells.[2] The latter has been demonstrated in a very recent experimental study[3] by significantly increasing the solar cell efficiency in colloidal Si NCs due to carrier multiplication (CM) which enables multiple exciton generation in response to a single absorbed photon.[4,5] Similarly, the inverse process, the Auger recombination (AR), is also operational and it introduces a competing mechanism to CM which can potentially diminish the solar cell efficiency and in the case of light sources, it degrades the performance by inflating the nonradiative carrier relaxation rate.[6]

The utilization and full control of both CM and AR require a rigorous theoretical understanding. The pioneering series of theory publications on the AR in Si NCs belong to a single group based on an atomistic tight binding approach.[7–9] Unfortunately, they only considered hydrogen-passivated Si NCs without addressing the shape effects. Moreover, their results do not reveal a size scaling for AR but rather a scattered behavior over a wide band of lifetimes in the range from a few picoseconds to a few nanoseconds as the NC diameter changes from 2 to 4 nm. In the past decade, no further theoretical assessment of AR in Si NCs was put forward. In this context, the Ge NCs have not received any attention although with their narrower effective band gap, they can benefit more from the low-energy part of the solar spectrum in conjunction with CM for increasing the efficiency.

In this work, we provide a theoretical account of AR and CM in Si and Ge NCs which reveals their size, shape, and energy dependence. Another important feature of this work, unlike commonly studied hydrogen-passivated NCs, is that we consider NCs *embedded* in a wide band-gap matrix which is essential for the solid-state device realizations. Similar to the classification of Wang *et al.* in their theoretical work on the Coulombic excitations in CdSe NCs,[10] we consider different possibilities of AR, as shown in Fig. 1. We use the type of the exicted carrier as the discriminating label, hence we have the excited electron [Fig. 1(a)] and the excited hole [Fig. 1(b)] AR and their biexciton variants [Figs. 1(c) and 1(d)]. All of these have corresponding CM processes taking place in the reverse direction, but only the CMs in Figs. 1(c) and 1(d) are studied as they can be optically induced.

II. THEORETICAL DETAILS

Both AR and CM require an accurate electronic structure over a wide energy band extending up to at least 3–4 eV

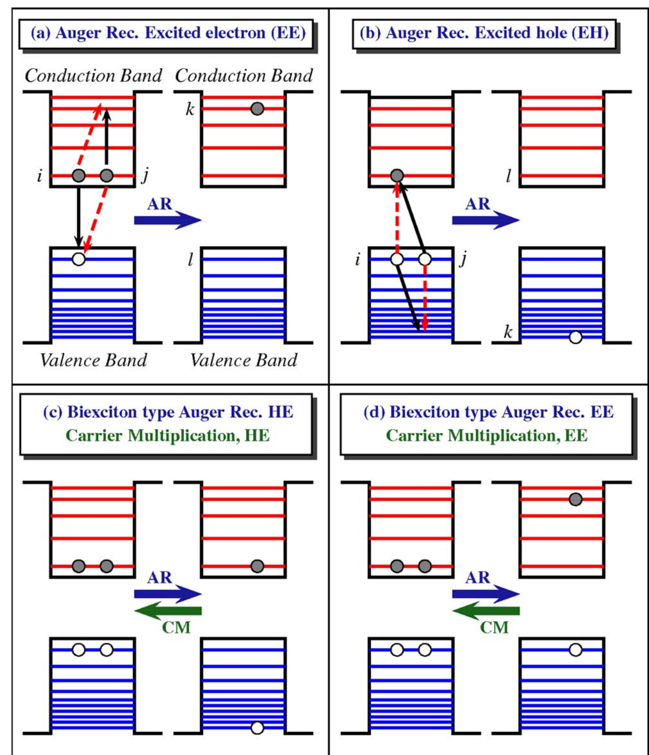

FIG. 1. (Color online) AR in NCs: (a) excited electron and (b) excited hole; the solid and dashed arrows refer to direct and exchange processes. Biexciton type AR and its inverse process CM: (c) excited electron and (d) excited hole.

 ©2008 The American Physical Society

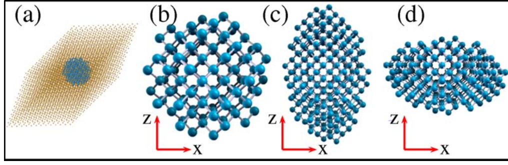

FIG. 2. (Color online) (a) Embedded NC in a supercell and core atoms of (b) spherical, (c) oblate, and (d) prolate ellipsoidal NCs.

below (above) the highest occupied molecular orbital (HOMO) [lowest unoccupied molecular orbital (LUMO)]. Another constraint is to incorporate several thousands of cores and host matrix atoms within a supercell [see Fig. 2(a)]. To meet these requirements, we have employed the linear combination of bulk band basis within the empirical pseudopotential framework which can handle thousands-of-atom systems both with sufficient accuracy and efficiency over a large energy window.[11] Details regarding its performance and the implementation such as the wide band-gap host matrix can be found in Ref. 12. We should mention that Califano *et al.* have successfully employed a very similar theoretical approach in order to explain the hole relaxation in CdSe NCs.[13]

After solving the atomistic empirical pseudopotential Hamiltonian for the energy levels and the wave functions, the AR and CM probability can be extracted using the Fermi golden rule,

$$R = \frac{\Gamma}{\hbar}\sum_f \frac{|\langle\psi_i|V_C(\mathbf{r}_1,\mathbf{r}_2)|\psi_f\rangle|^2}{(E_f-E_i)^2+(\Gamma/2)^2}, \tag{1}$$

where ψ_i and ψ_f are respective initial and final configurations with the corresponding energies E_i and E_f, respectively, and Γ is the level broadening parameter which is taken as 10 meV. However, sensitivity to this parameter is also considered in this work. The spin-conserving screened Coulomb potential is given by $V_C(\mathbf{r}_1,\mathbf{r}_2)=e^2/\epsilon(\mathbf{r}_1,\mathbf{r}_2)|\mathbf{r}_1-\mathbf{r}_2|$. The subject of the screened Coulomb interaction in NCs is an active source of debate; recent publications predict reduced screening,[14,15] whereas other theoretical investigations[10,16] have concluded that the inverse dielectric function is bulk-like inside the NC. Therefore, we follow[10] and use

$$\frac{1}{\epsilon(\mathbf{r}_1,\mathbf{r}_2)} = \frac{1}{\epsilon_{\text{out}}} + \left(\frac{1}{\epsilon_{\text{in}}}-\frac{1}{\epsilon_{\text{out}}}\right)m(\mathbf{r}_1)m(\mathbf{r}_2), \tag{2}$$

as the inverse dielectric function, where the so-called mask function $m(\mathbf{r})$ is set to 1 when $\mathbf{r}$ is inside of the NC and 0 when $\mathbf{r}$ is outside of the NC.

Expressing the initial and final states of the AR shown in Fig. 1(a) or 1(b) by using the Slater determinant, the matrix elements $[\langle\psi_i|V_C(|\mathbf{r}_1,\mathbf{r}_2|)|\psi_f\rangle]$ can be calculated as

$$M(i,j;k,l) = \frac{1}{V^2}\int\int \phi_k^*(\mathbf{r}_1)\phi_l^*(\mathbf{r}_2)V_C(\mathbf{r}_1,\mathbf{r}_2) \times[\phi_i(\mathbf{r}_1)\phi_j(\mathbf{r}_2)-\phi_j(\mathbf{r}_2)\phi_i(\mathbf{r}_1)]d^3r_1d^3r_2, \tag{3}$$

where labels i, j and k, l refer, respectively, to the initial and final states which also include the spin and V is the volume of the supercell.

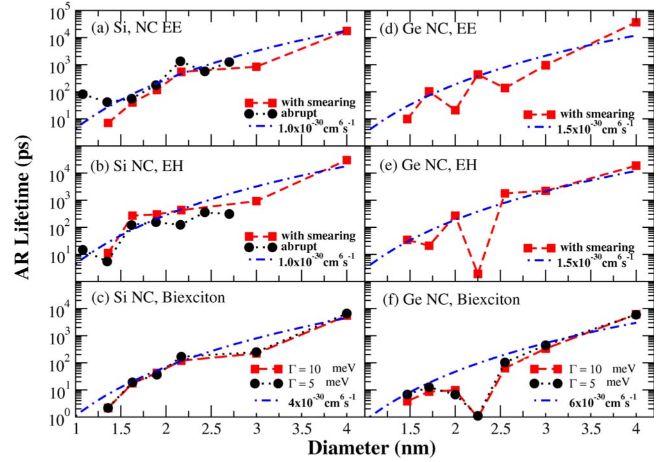

FIG. 3. (Color online) AR lifetimes for (a) excited electron, (b) excited hole, and (c) biexciton types in Si NCs, and (d) excited electron, (e) excited hole, and (f) biexciton types in Ge NCs. Square symbols represent AR lifetimes with interface smearing, and dashed lines show AR lifetimes calculated from our proposed C values. Spherical symbols in (a) and (b) represent AR lifetimes in Si NCs with abrupt interfaces.

These matrix elements, $M(i,j;k,l)$, are computed exactly in a three-dimensional real space grid without resorting to any envelope approximation. A number of final states are determined setting the final state window to $\pm 7\Gamma$ around the exact conserved energy $E_k(=E_j+E_i-E_l)$. For the initial states i and l, the Boltzmann average is taken into account due to thermal excitations. The same should apply to the other initial state j, however, as a safe but computationally very rewarding simplification, it is kept fixed at LUMO for the excited electron (EE) and at HOMO for the excited hole (EH) type AR.

III. RESULTS AND DISCUSSIONS

We first apply this formalism to spherical NCs [see Fig. 2(b)] having abrupt interfaces. The corresponding AR lifetimes for EE and EH processes are plotted as a function of NC diameter in Figs. 3(a) and 3(b). The C_{3v} point symmetry of the NCs in the case of abrupt interface between NC core and the matrix causes oscillations in the physical quantities such as the state splittings and the density of states with respect to NC diameter.[12] When we account for the interface transition region between the NC and host matrix,[17] we observe that these strong oscillations in the size dependence of AR are highly reduced for Si and Ge NCs (cf. Fig. 3). The interface region especially affects the excited state wave functions and the final state density of states and it makes our model more realistic for both Si and Ge NCs. As an observation of practical importance, we can reproduce our data remarkably well (cf. Fig. 3) using the simple expression $1/\tau=Cn^2$, with Auger coefficients $C=1\times10^{-30}$ cm^6 s^{-1} for Si NCs and $C=1.5\times10^{-30}$ cm^6 s^{-1} for Ge NCs, where $n=2/V_{\text{NC}}$ is the carrier density within the NC such that there

TABLE I. AR lifetimes for different ellipsoidal shapes of Si NCs with diameters of 1.63 and 2.16 nm.

	Spherical		Prolate		Oblate	
D (nm)	1.63	2.16	1.63	2.16	1.63	2.16
EE (ps)	40	541	32	103	36	121
EH (ps)	267	430	74	76	26	139

should be two electrons or holes to initiate an AR.

The other two types of AR shown in Figs. 3(c) and 3(f) refer to biexciton recombinations. This process becomes particularly important under high carrier densities such as in NC lasers or in solar cells under concentrated sunlight. Its probability can be expressed in terms of EE and EH type AR as[10] $1/\tau_{XX}=2/\tau_{\mathrm{EE}}+2/\tau_{\mathrm{EH}}$, where τ_{EE} and τ_{EH} are EE and EH lifetimes. Figures 3(c) and 3(f) compare the computed biexciton type AR for Si and Ge NCs with the expression $1/\tau=Cn^2$, where values $C=4\times10^{-30}$ and 6×10^{-30} cm^6 s^{-1} are used, which are obtained from the previous C values extracted for EE and EH processes together with the τ_{XX} expression. For Si NC case, our calculated value at 3 nm diameter agrees reasonably well with the experimental photoluminescense decay time of about 105 ps which was attributed to AR.[18] In Figs. 3(c) and 3(f), we also demonstrate the fact that a choice of $\Gamma=5$ meV does not introduce any marked deviation from the case of $\Gamma=10$ meV as used in this work for both Si and Ge NCs. This parameter test automatically checks the sensitivity to the final state energy window chosen as $\pm7\Gamma$.

Next, we demonstrate the effects of deviation from sphericity on Si NCs. We consider both oblate [Fig. 2(c)] and prolate [Fig. 2(d)] ellipsoidal Si NCs described by the ellipticity value of $e=0.85$. For the comparison purposes, we preserve the same number of atoms used in spherical NCs with diameters of 1.63 and 2.16 nm. The results listed in Table I indicate that the spherical NC has a lower Auger rate than the aspherical shapes. This can be reconciled as follows: in the case of either prolate or oblate NC, the electronic structure is modified in such a way that the number of final states is increased, furthermore, a coalescence of the states around the HOMO and LUMO occurs. A similar effect was also observed in the asphericity-induced enhancement of the Auger thermalization of holes in CdSe NCs.[13] However, we should note that the shape effects are not pronounced.

In their work, on the CM in PbSe NCs, Allan and Delerue have deduced that such Coulombic interactions are primarily

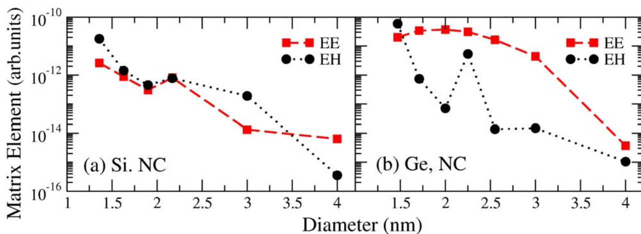

FIG. 4. (Color online) Average Coulomb matrix elements for (a) Si and (b) Ge NCs for EE type AR (red/gray squares) and for EH type AR (black spheres).

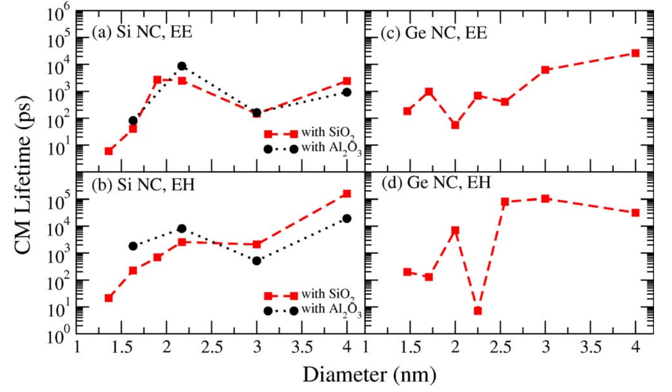

FIG. 5. (Color online) CM lifetime results for (a) EE and (b) EH types in Si NCs embedded in SiO_2 and Al_2O_3, and (c) EE and (d) EH types in Ge NCs embedded in Al_2O_3.

governed by the state-density function.[19] Even though we agree on the importance of the density of states, we would like to emphasize the significant role of the Coulomb matrix elements. We illustrate our point in Fig. 4, where the average matrix elements for Si and Ge NCs are shown. The strong size dependence leading to a variation over several orders of magnitude indicates their nontrivial role.

Regarding the CM, we first consider the inverse Auger process [cf., Figs. 1(c) and 1(d)] for different diameters of the Si and Ge NCs. Therefore, we consider the impacting electron (hole) to have an energy of $E_{\mathrm{gap}}=E_{\mathrm{LUMO}}-E_{\mathrm{HOMO}}$ above (below) the conduction (valence) band edge, i.e., just at the threshold energy to initiate a CM event. As seen in Fig. 5, EE- and EH-type CM lifetimes for Si and Ge NCs decrease from the few nanoseconds to few picoseconds as the NC diameter decreases. However, for EE- (EH-) type CM, a small number of final states at the bottom of the conduction band (top of the valence band) cause a nonmonotonic dependence of CM on the size of the NC.

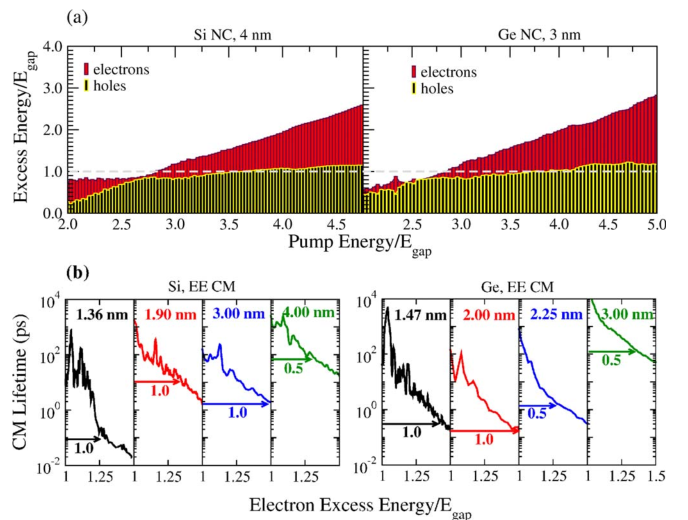

FIG. 6. (Color online) (a) Electron and hole excess energy vs optical pump (excitation) energy for 4 nm Si and 3 nm Ge NCs. (b) CM lifetime vs electron excess energy for different diameter of Si and Ge NCs. The horizontal arrows provide the 1 and 0.5 eV marks.

From the practical point of view, the investigation of the effect of excess energy on the CM under an optical excitation above the effective gap E_{gap} is even more important. Here, the correct placement of excited electron and hole after optical excitation is critical. We assign the excited electron and hole to their final states by accounting for all interband transitions with the given energy difference as weighted by the dipole oscillator strength of each transition which is a direct measure of the probability of that particular event. In Fig. 6(a), we observe that the electrons receive the lion's share of the total excess energy which is the desired case for the high efficiency utilization of CM in photovoltaic applications.[20] Our threshold value of $2.8E_{gap}$ for Si NCs is somewhat higher than the recent experimental data.[3] In Fig. 6(b), we show the corresponding electron-initiated CM lifetimes as a function of excess energy. It can be observed that CM is enhanced by more than 2 orders of magnitude within an excess energy of 1 eV beyond the CM threshold reaching a lifetime of a few picoseconds.

IV. CONCLUSIONS

To summarize, we offer a theoretical assessment of the two most important Coulombic excitations, AR and CM, in Si and Ge NCs. The Auger coefficients that we extracted can serve for the practical needs in the utilization of this process. For the efficiency enhancement via CM in Si and Ge NCs, the prospects look positive as the hot electrons receive most of the excess energy and they can undergo a CM within a few picoseconds.

ACKNOWLEDGMENTS

This work has been supported by the European FP6 Project SEMINANO under the Contract No. NMP4 CT2004 505285 and by the Turkish Scientific and Technical Council TÜBİTAK with the Project No. 106T048. The computational resources are supplied in part by TÜBİTAK through TR-Grid e-Infrastructure Project.

[1] S. Ossicini, L. Pavesi, and F. Priolo, *Light Emitting Silicon for Microphotonics* (Springer-Verlag, Berlin, 2004).
[2] M. C. Hanna and A. J. Nozik, J. Appl. Phys. **100**, 074510 (2006).
[3] M. C. Beard, K. P. Knutsen, P. Yu, J. M. Luther, Q. Song, W. K. Metzger, R. J. Ellingson, and A. J. Nozik, Nano Lett. **7**, 2506 (2007).
[4] R. D. Schaller and V. I. Klimov, Phys. Rev. Lett. **92**, 186601 (2004).
[5] R. J. Ellingson, M. C. Beard, J. C. Johnson, P. Yu, O. I. Micic, A. J. Nozik, A. Shabaev, and A. L. Efros, Nano Lett. **5**, 865 (2005).
[6] V. I. Klimov, J. Phys. Chem. B **110**, 16827 (2006).
[7] I. Mihalcescu, J. C. Vial, A. Bsiesy, F. Muller, R. Romestain, E. Martin, C. Delerue, M. Lannoo, and G. Allan, Phys. Rev. B **51**, 17605 (1995).
[8] C. Delerue, M. Lannoo, G. Allan, E. Martin, I. Mihalcescu, J. C. Vial, R. Romestain, F. Muller, and A. Bsiesy, Phys. Rev. Lett. **75**, 2228 (1995).
[9] M. Lannoo, C. Delerue, and G. Allan, J. Lumin. **70**, 170 (1996).
[10] L. W. Wang, M. Califano, A. Zunger, and A. Franceschetti, Phys. Rev. Lett. **91**, 056404 (2003).
[11] L. W. Wang, A. Franceschetti, and A. Zunger, Phys. Rev. Lett. **78**, 2819 (1997).
[12] C. Bulutay, Phys. Rev. B **76**, 205321 (2007).
[13] M. Califano, G. Bester, and A. Zunger, Nano Lett. **3**, 1197 (2003).
[14] S. Öğüt, R. Burdick, Y. Saad, and J. R. Chelikowsky, Phys. Rev. Lett. **90**, 127401 (2003).
[15] F. Trani, D. Ninno, G. Cantele, G. Iadonisi, K. Hameeuw, E. Degoli, and S. Ossicini, Phys. Rev. B **73**, 245430 (2006).
[16] G. Allan, C. Delerue, M. Lannoo, and E. Martin, Phys. Rev. B **52**, 11982 (1995).
[17] N. Daldosso, M. Luppi, S. Ossicini, E. Degoli, R. Magri, G. Dalba, P. Fornasini, R. Grisenti, F. Rocca, L. Pavesi, S. Boninelli, F. Priolo, C. Spinella, and F. Iacona, Phys. Rev. B **68**, 085327 (2003).
[18] F. Trojánek, K. Neudert, M. Bittner, and P. Malý, Phys. Rev. B **72**, 075365 (2005).
[19] G. Allan and C. Delerue, Phys. Rev. B **73**, 205423 (2006).
[20] J. H. Werner, S. Kolodinski, and H. J. Queisser, Phys. Rev. Lett. **72**, 3851 (1994).